Distinct anticancer properties of exosomes from induced mesenchymal stem cells vs. bone marrow-derived stem cells in MCF7 and A549 models

NIDAA A. ABABNEH[1], RAZAN ALDIQS[1*], SURA NASHWAN[1*], MOHAMMAD A. ISMAIL[1], RAGHDA BARHAM[1], SABAL AL HADIDI[1], AYA ALREFAE[1], FARAH K. ALHALLAQ[1], ANAS HA ABU-HUMAIDAN[2], TAREQ SALEH[3,4] and ABDALLA AWIDI[1,5,6]

[1]Cell Therapy Center, The University of Jordan, Amman 11942, Jordan; [2]Department of Pathology, Microbiology and Forensic Medicine, School of Medicine, The University of Jordan, Amman 11942, Jordan; [3]Department of Pharmacology and Public Health, Faculty of Medicine, The Hashemite University, Zarqa 13133, Jordan; [4]Department of Pharmacology and Therapeutics, College of Medicine and Health Sciences, Arabian Gulf University, Manama 26671, Bahrain; [5]Hemostasis and Thrombosis Laboratory, School of Medicine, The University of Jordan, Amman 11942, Jordan; [6]Department of Hematology and Oncology, Jordan University Hospital, Amman 11942, Jordan

Received October 23, 2024; Accepted April 15, 2025

DOI: 10.3892/br.2025.1994

Abstract. Mesenchymal stem cells (MSCs) have significant potential in regenerative medicine due to their multipotency, however, they face clinical challenges such as limited expansion and heterogeneity. Induced pluripotent stem cell-derived MSCs (iMSCs) are promising alternatives. The present study compared the effects of exosomes from bone marrow stromal MSCs (BMSCs) and iMSCs on A549 and MCF7 cancer cells to explore the unique properties of iMSCs. Proliferation assays revealed that both exosome types inhibited MCF7 and A549 cell proliferation at 24 h ($P \leq 0.0001$ for both) compared with the control, with BMSC-exosomes (Exos) exerting a more significant effect on MCF7 cells ($P \leq 0.01$). After 48 h, the significant effects of the BMSC-Exos were no longer observed on either cell line, whereas the iMSC-Exos continued to suppress A549 cell proliferation ($P \leq 0.001$ compared with the control; $P \leq 0.01$ compared with BMSC-Exos), indicating a longer-lasting effect. An investigation of senescence-associated β-galactosidase (SA-βGal) activity revealed no significant effect on senescence induction in MCF7 cells treated with either type of exosomes. By contrast, compared with the control treatment, the treatment of A549 cells with exosomes resulted in a significant increase in the number of senescent cells ($P \leq 0.0001$). While the apoptosis assay performed by flow cytometry revealed no significant effect on apoptosis, this increase in senescence aligned with the decreased proliferation observed in A549 cells, indicating that the antitumor effect of the exosomes on A549 cells was mediated partially through the induction of senescence. Wound healing assays revealed that BMSC-Exos significantly increased the migration of MCF7 cells at 20 h ($P \leq 0.01$). However, this effect was reversed at 47 h ($P \leq 0.05$), indicating a time-dependent effect of BMSC-Exos. In A549 cells, no significant difference in migration was observed after treatment with either exosome preparation. These findings highlight the distinct effects of iMSC- and BMSC-derived exosomes on cancer cells, emphasizing the need for further investigations into their therapeutic potential and underlying mechanisms.

Correspondence to: Dr Nidaa A. Ababneh or Professor Abdalla Awidi, Cell Therapy Center, The University of Jordan, Queen Rania Street, Amman 11942, Jordan
E-mail: n.ababneh@ju.edu.jo
E-mail: aabbadi@ju.edu.jo

*Contributed equally

Key words: bone marrow-derived mesenchymal stem cells, cell-free therapy, exosomes, induced mesenchymal stem cells, breast cancer, lung cancer

Introduction

Recent statistics highlighted the ongoing global burden of cancer. In the United States alone, cancer continues to pose a significant threat to human health, with ~2 million new cancer cases and over 600,000 cancer-related deaths projected in 2024, emphasizing the critical need for improved diagnostic and therapeutic strategies (1). The incidence rates of several cancers, including breast cancer, have steadily increased in recent years. Specifically, the number of breast cancer cases rose by 0.6-1% annually between 2015 and 2019, reflecting its increasing prevalence and the urgent need for improved prevention and treatment strategies (1). Moreover, in 2024, lung cancer, along with prostate and colorectal cancers, accounted for 48% of cases in men, whereas in women, lung, breast, and colorectal cancers comprised 51% of diagnoses (1).

Cancer therapy has advanced from conventional methods such as chemotherapy to personalized treatments such as chimeric antigen receptor T-cell therapy, antibody-drug conjugates and bispecific T-cell engagers; however, improved treatments are continually pursued (2).

The capacity of stem cells to self-renew and develop into other types of cells makes them a potential source for regenerative medicine (3). Stem cells are classified into totipotent, pluripotent, multipotent and unipotent stem cells based on their differentiation potential (4). Mesenchymal stem cells (MSCs) are obtained from various organs and tissues, including the brain, liver, kidney, lung, muscle, thymus, pancreas, skin, adipose tissue, fetal tissue, umbilical cord, Wharton's jelly (WJ) and placenta (5). Bone marrow stromal MSCs (BMSCs) are a subset of multipotent adult stem cells that are derived primarily from the bone marrow and play a crucial role in osteogenesis by differentiating into osteoblasts, which are responsible for bone formation (6). BMSCs are the most common type of MSCs used in cell therapy and tissue repair (7). MSCs must meet the following criteria as outlined by the International Society for Cellular Therapy (ISCT): i) MSCs must express specific surface markers including, CD105, CD90, and CD73; ii) they must not express other surface markers such as CD45, CD34, CD14 or CD11b, CD79α or CD19, and HLA-DR (8); iii) they must adhere to plastic in culture conditions; and iv) they be able to differentiate into adipocytes, chondrocytes, and osteoblasts *in vitro* (8).

MSCs are considered promising sources for cell therapy in regenerative medicine (7). However, several significant challenges limit their potential for therapeutic applications, including their limited ability to expand efficiently (9). Furthermore, MSCs are inherently heterogeneous and display diverse biological properties that contribute to inconsistent outcomes in clinical trials (10). This heterogeneity is attributed to differences in donor characteristics, tissue sources, cell surface markers and variations in microenvironmental and culture conditions (10). As a result, an increasing demand for alternative cell sources that can address these limitations and enhance the effectiveness of cell therapy using MSCs has been noted.

Adult somatic cells can be effectively converted into undifferentiated cells, known as induced pluripotent stem cells (iPSCs) (11,12). These iPSCs share similar characteristics with embryonic stem cells (ESCs) (13). Notably, iPSCs have a high capacity for self-renewal and pluripotent differentiation, allowing them to develop into a variety of cell types, such as MSCs, neurons, and cardiomyocytes (14). Compared with conventional MSCs, iPSC-derived MSCs (iPSC-MSCs) have been shown to exhibit superior cellular viability, including enhanced survival, proliferation, and differentiation abilities. These properties are due to a rejuvenation process that occurs during reprogramming (15,16). The rejuvenation of iPSCs may also reduce the heterogeneity typically associated with MSCs, which is often influenced by the tissue source and donor age, thereby providing a more consistent and reliable cell source for therapeutic applications (16).

One of the primary challenges facing cell therapy is the effective delivery of cells to damaged tissues (5). Although studies have revealed that labeled MSCs delivered *in vivo* can migrate to injured tissues, such as brain lesions or cardiac infarcts, only a small number of MSCs engraft at the injury sites (17-19). However, the paradigm has shifted toward the hypothesis that MSCs influence host cells primarily through their paracrine factors (20,21). The culture medium conditioned by MSCs, known as conditioned medium (MSC-CM), contains a multitude of bioactive soluble factors secreted by MSCs, including growth factors, cytokines, chemokines, enzymes, and extracellular vesicles (EVs) (22,23). MSC-CM is considered a preferred option for use in cell therapy due to several key advantages over cell-based applications: i) It avoids the risk of host immune reactions; ii) it can be stored for relatively long periods without the use of toxic cryopreservatives such as DMSO; iii) it is cost-effective; and iv) the process of evaluating the safety and efficacy of MSC-CM is considerably simpler than that of conventional pharmaceutical agents or MSCs (21). MSC-derived extracellular vesicles (MSC-EVs) have garnered significant attention due to their primary role in mediating cellular communication (24). MSC-EVs also modify the activity of target cells by transferring mRNAs, microRNAs (miRNAs or miRs), lipids, and proteins (25).

The therapeutic importance of EVs, and their ability to modulate target cells and enhance tissue repair, has been previously demonstrated (26). Traditionally, EVs are classified into three subtypes based on their size and biogenesis, namely, exosomes, microvesicles (MVs), and apoptotic bodies (27-29). However, some studies have categorized apoptotic bodies, exosomes and exosome-like vesicles as distinct types of EVs, whereas other studies have focused only on microvesicles and exosomes due to a lack of sufficient evidence supporting the classification of other types of EVs (30,31).

EVs are heterogeneous membranous structures that originate from the endosomal system or are shed from the plasma membrane and are secreted by cells through different mechanisms (32). EVs are composed of different subtypes, primarily exosomes and microvesicles, which vary in size, origin, and content (33,34). Exosomes are nanosized vesicles ranging from 30 to 200 nm in diameter that contain proteins, mRNAs, and miRNAs (35,36). They play key roles in various cancer-related biological processes, such as angiogenesis, metastasis, and immune system regulation, and influence the tumor microenvironment (37). Moreover, MSC-derived exosomes have been utilized in engineered systems for targeted delivery, enhancing therapeutic efficacy in various diseases and tissue regeneration applications (38-40).

MSC-exosomes (Exos) including BMSC-Exos have been studied for their potential in cancer therapy, particularly as a delivery system for therapeutic molecules, with numerous studies focusing on their effects on tumor progression and the treatment response. For example, Zhou *et al* (41) demonstrated that BM-MSC-derived exosomes loaded with paclitaxel and gemcitabine monophosphate improved drug delivery and efficacy in PDAC, addressing chemoresistance and ECM abnormalities. Lin *et al* (42) reviewed the role of MSC-Exos in shaping the tumor microenvironment and driving therapy resistance, providing insights into their molecular mechanisms and clinical applications. In breast cancer, MSC-EVs modulated stemness markers (OCT4 and ALDH1) and proliferation in a concentration-dependent manner in MCF7 cells (43). In lung cancer, BMSC-Exos promoted invasion, migration, and metastasis by delivering miR-425 which suppressed cytoplasmic

polyadenylation binding protein 1 (CPEB1) expression (44). Together, these findings highlight the therapeutic potential of MSC-Exos across various cancer models.

Moreover, Zhao *et al* (45) described the therapeutic potential of induced pluripotent stem cell-derived MSC (iMSC)-Exos in enhancing treatment responses in metastatic prostate cancer, highlighting the potential role of iMSC-Exos as anticancer agents. However, in contrast to that of BMSC-Exos, the role of iMSC-Exos in cancer therapy remains less explored. The present study focused on comparing the effects of BMSC-Exos and iMSC-Exos on MCF7 and A549 cancer models. The MCF7 cell line, a widely recognized model of human breast cancer, has been used extensively in advancing therapeutic strategies and exploring cancer biology (46,47). Similarly, the A549 cell line, a model of non-small cell lung cancer, has been pivotal for exploring cancer treatments and their underlying biology (48-50). The present study explored the effects of exosomes derived from BMSCs and iMSCs on lung and breast cancer, specifically the A549 lung cancer and MCF7 breast cancer cell lines.

Material and methods

Cell culture. In the present study, BMSCs were previously isolated from 2 male and 2 female non-smoking patients (25-45 years old), who were referred to the Orthopedic Department of Jordan University Hospital (JUH)/University of Jordan (Amman, Jordan) after sustaining orthopedic fractures from road traffic accidents (51). Institutional Review Board (IRB) approval (approval no. IRB/7/2019) for obtaining BMSCs was issued by the IRB Committee of the Cell Therapy Center (CTC)/University of Jordan. Informed consent was also obtained from all patients to donate their tissues, as specified in The Declaration of Helsinki, prior to participation.

Bone marrow samples were collected by iliac crest aspiration. The inclusion criteria for patient selection were as follows: i) Males or females, 25-45 years old; ii) those with orthopedic fractures or trauma resulting from traffic accidents requiring orthopedic intervention, in which iliac crest bone marrow aspiration did not pose any additional risk; and iii) hemodynamically stable (normal vital signs or stabilized post-resuscitation). While the exclusion criteria were as follows: i) History of, or evidence of, hematologic disorders, including leukemia, lymphoma, or aplastic anemia; ii) major mental health disorders that preclude participation in the present study; iii) type I or type II diabetes mellitus, chronic hypertension, or receiving antidiabetic medications; iv) severe anemia (hemoglobin <8 g/dl); v) active systemic infection (such as sepsis and osteomyelitis) that may contaminate the bone marrow; vi) a clinically active autoimmune condition; vii) history of chemotherapy or radiation therapy, which may alter bone marrow cell composition; and viii) positive serological evidence of HIV I and II, HBV, HCV, and VDRL.

All participants met the inclusion criteria and had none of the exclusion conditions, confirming their suitability for the present study.

Bone marrow sample collection began on December 1, 2019, and continued for 1 year until January 1, 2021. Bone marrow samples were aseptically collected in 12-16 EDTA tubes. Subsequently, the buffy coat was isolated by centrifugation [300 x g, 6 min, at room temperature (RT)], suspended in 1.5 ml phosphate-buffered saline (PBS), and used for culture. Then, 5 ml of the separated buffy coat was layered onto an equal volume of Ficoll (Cytiva) and centrifuged (500 x g, 30 min, at RT with the centrifuge brake turned to off).

For the present study, all the experimental procedures were approved (approval no. IRB-7-2019-8) by the IRB Committee at the CTC, University of Jordan. BMSCs were cultured at passage 3 in minimum essential medium Eagle-alpha modification (αMEM; Gibco; Thermo Fisher Scientific, Inc.) supplemented with 15% fetal bovine serum (FBS; Cytiva), 1% of 100X Glutamax (Gibco; Thermo Fisher Scientific, Inc.), and 1% of 100X antibiotic-antimycotic mixture (Gibco; Thermo Fisher Scientific, Inc.). Breast cancer (MCF7, ATCC® HTB-22™) and alveolar basal epithelial adenocarcinoma (A549, ATCC® CCL-185™) were cultured in RPMI-1640 medium (Gibco; Thermo Fisher Scientific, Inc.) supplemented with 10% FBS, 1% of 100X Glutamax, and 1% of 100X antibiotic-antimycotic. Moreover, human dermal fibroblast cells used were previously prepared (49,50) and cultured in Advanced DMEM (Gibco; Thermo Fisher Scientific, Inc.) supplemented with 10% FBS, 1% of 100X Glutamax, and 1% of 100X antibiotic-antimycotic mixture. All cells were maintained and incubated at 37˚C, 21% O_2, and 5% CO_2, with media changes every 2 days.

Generation of embryoid body-derived iMSCs (EB-iMSCs). The four iPSC lines used in the present study are as follows: JUCTCi010-A, derived from skin dermal fibroblasts of a healthy 27-year-old Jordanian female (49); JUCTCi010-B, derived from MSCs obtained from skin dermal fibroblasts of a 27-year-old Jordanian female (49); JUCTCi011-A and JUCTCi011-B, derived from skin dermal fibroblasts of a 34-year-old Jordanian male (50). The generation of these lines was approved (approval no. IRB/07/2017) by the Cell therapy Center (CTC), University of Jordan, Amman, Jordan, which covered JUCTCi010-A and B as well as JUCTCi011-A and B. This IRB approval has been documented in previous publications by the authors on female (52) and male (53) iPSC lines.

For coating plates used to culture iPSCs in mTeSR media (STEMCELL Technologies), Matrigel was diluted 1:100 in DMEM/F12 to achieve a final concentration of ~500 μg/ml. For a 6-well plate, 1 ml of the diluted Matrigel solution was added per well and incubated for at least 1 h at 37˚C before use (51). For differentiation, the iPSC monolayer cultures were detached using 0.5 M EDTA (Gibco; Thermo Fisher Scientific, Inc.), and the resulting cell suspensions were plated in MSC differentiation media on ultra-low attachment plates to form EBs (54). The MSC differentiation media consisted of αMEM, supplemented with 15% FBS, 1% 100X Glutamax, and 1% 100X antibiotic-antimycotic mixture (54).

On days 2 and 4 of differentiation, the media were replaced with fresh media containing 10 μM retinoic acid (RA; Merck KGaA) and 0.1 μM RA, respectively. On day 6, the media were switched to RA-free differentiation media and on day 7, the EBs were plated on Matrigel-coated plates and maintained in MSC differentiation media. The differentiation media were replaced every two days. On day 12, 2.5 ng/ml basic fibroblast growth factor (R&D Systems, Inc.) was added, with media changes occurring every 2 days thereafter. iMSCs were passaged upon reaching 80-90% confluency and were then cryopreserved in

1X freezing media composed of 90% FBS and 10% DMSO and stored in liquid nitrogen.

Osteogenic differentiation. Cells were seeded in triplicate at a density of 200,000 cells per well in 6-well plates and cultured in complete culture medium (CCM) until reaching 50% confluency. The medium was then replaced with osteogenic differentiation medium consisting of αMEM supplemented with 15% FBS, 1% 100X Glutamax, 1% 100X antibiotic-antimycotic mixture, 10 mM dexamethasone (Merck KGaA), 50 μg/ml ascorbic acid 2-phosphate (Merck KGaA), and 10 mM β-glycerophosphate (Carbosynth Ltd.) for 21-28 days, or until calcium deposits appeared. Control cells remained in CCM with medium changes every 2-3 days. Upon observation of mineral deposits, one well from each sample was stained with Alizarin Red (Merck KGaA) for 5 min at RT to visualize calcium deposits, which were then imaged using the EVOS XL Core Imaging System (Thermo Fisher Scientific, Inc.).

Adipogenic differentiation. EB-iMSCs and BMSCs were seeded in triplicate at a density of 200,000 cells per well and cultured in CCM until reaching 50% confluency. They were then switched to adipogenic differentiation medium consisting of αMEM supplemented with 15% FBS, 1% 100X Glutamax, 1% 100X antibiotic-antimycotic mixture, 10 mM dexamethasone, 500 μM 3-isobutyl-1-methylxanthine (IBMX), 0.2 mM indomethacin, and 10 μg/ml insulin (all from Merck KGaA) and maintained for 14-21 days, with medium changes every 2-3 days, until fat vacuoles were visible. Control cells remained in CCM. Upon differentiation, the cells were stained with Oil Red-O (Merck KGaA) for 5 min at RT to visualize fat vacuoles, which were then imaged using the EVOS XL Core Imaging System.

Flow cytometry of iMSC and human (h)MSC surface markers. Cells were assessed by flow cytometry using BD Stem Flow hMSC Analysis kit (cat. no. 562245, BD Biosciences) and according to the manufacturer's instructions. iMSCs and BMSCs were trypsinized at early passages (passage <8) and washed with 1X PBS. The cells were then resuspended in 800 μl of 1% bovine serum albumin (BSA) staining buffer. Next, the cells were incubated for 30 min with fluorescently conjugated antibodies targeting human MSC surface markers (FITC anti-CD90, PerCP anti-CD105, APC anti-CD73, and PE anti-CD44; all included in th aforementioned kit) or with appropriate isotype controls (all from BD Biosciences) at a concentration of 50 μg/ml for FITC anti-CD90, PerCP anti-CD105, and APC anti-CD73, and 20 μg/ml for anti-CD44 and the isotype controls. The absence of negative cocktail surface markers was also. Following incubation, the cells were washed twice with 1X PBS to remove any unbound antibodies and then resuspended in 200 μl of PBS. The expression of surface markers was analyzed using a BD FACSCanto II flow cytometer (BD Biosciences), and the data were processed using BD FACSDiva software (BD Biosciences) (55).

Exosome preparation. After reaching 70-80% confluency, cells of iMSCs and BMSCs at passage 3 were washed with PBS and then cultured in serum-free α-MEM for 48 h. The conditioned media were then collected and centrifuged at 300 x g for 10 min at 4˚C, followed by centrifugation in 2,000 x g for 20 min at 4˚C. Following centrifugation, the supernatants were filtered through 0.22-μm filter units to remove any remaining cell debris, which could contribute to exosome aggregation during the filtration process. To ensure consistent exosome pelleting, the filtered supernatant was then ultracentrifuged at 110,000 x g for 2 h at 4˚C using a fixed-angle rotor. After purification, the exosome pellets (iMSC-Exos and BMSC-Exos) were gently resuspended in 500 μl filtered PBS to avoid disrupting the lipid bilayer, which could promote aggregation. The concentration of the exosomes was measured using the Micro BCA™ Protein Assay Kit (cat. no. 23235; Thermo Fisher Scientific, Inc.), strictly following the manufacturer's instructions. The measured concentration was standardized to 1 mg/ml. The exosomes were then aliquoted, resuspended in filtered PBS, and stored at -80˚C to preserve their structural integrity and reduce aggregation over time for future use (56).

iMSC-Exos and BMSC-Exos surface markers analysis. A total of ~100 μg of isolated exosomes were incubated with 3 μl of aldehyde/sulfate latex beads (4% w/v, 4 μm, Invitrogen; Thermo Fisher Scientific, Inc.) (57) for 15 min and then incubated overnight at RT with gentle shaking (270˚ shaking) after adding 10 μl of filtered 1X PBS. Subsequently, the exosome-bead binding was blocked by adding 1M glycine for 15 min at RT, which was prepared by dissolving 0.7507 g of 0.01 M glycine (Millipore, Sigma), 200 mg of 2% BSA (Abcam), and 10 ml of 1X PBS, followed by filtration using 0.22 μm filter units. The exosome-coated beads were then incubated for 40 min at 37˚C with various antibodies (A5488 anti-CD9 (cat. no. FAB1880G), AF647 anti-CD81 (cat. no. FAB4615R), and APC anti-CD63 (cat no. FAB5417A) or their respective isotype controls (all from BioTechne; R&D Systems, Inc.) according to the manufacturer's instructions. Finally, 150 μl of filtered 1X PBS was added to the samples, which were then processed on a BD FACSCanto II and analyzed using BD FACSDiva software.

Transmission electron microscopy (TEM). A total of 100 μg of purified exosomes were mixed 1:1 with 2% paraformaldehyde (PFA; MilliporeSigma), and applied to Formvar-carbon-coated electron microscopy grids [Electron Microscopy Sciences (EMS)] to promote membrane absorption for 20 min in a dry environment at RT. The grids were then rinsed with 1X PBS and subsequently immersed in 1% glutaraldehyde for 5 min at RT to eliminate any negative background. Following this, the grids were washed seven times with distilled water, with each wash lasting 2 min. To enhance contrast, the grids were treated with uranyl oxalate for 5 min at RT and then placed on methyl cellulose-UA for 10 min on ice. Finally, the grids were allowed to air dry for 10 min at RT before being examined under TEM with a magnification of 500 nm at an acceleration voltage of 30 kV, using VERSA 3D (FEI; Thermo Fisher Scientific, Inc.).

Size distribution measurement of exosomes. Size distribution was measured using a dynamic light scattering (DLS) nanosizer, the ZetaView (serial no. MAL1137709) (Malvern Nano ZS; Malvern Panalytical, Ltd.), which analyzes particle sizes ranging from 0.3 nm to 10 μm. Data were processed using Zetasizer software version 7.11 (Malvern Panalytical,

Ltd.). The temperature was maintained at 24˚C throughout the process. The data acquisition settings were configured as follows: A measurement angle of 173˚ backscatter, 10 runs per measurement, 60 sec per run, 3 total measurements, and a 10-sec delay between measurements. All settings followed the manufacturer's recommendations for EV analysis. Prior to measurement, samples were diluted with filtered PBS.

Cellular uptake of exosomes. iMSC-Exos and BMSC-Exos were labeled with 1,1'-dioctadecyl-3,3,3',3'-tetramethylindocarbocyanine perchlorate (DiI-O; Thermo Fisher Scientific, Inc.) fluorescent dye according to the manufacturer's instructions. Briefly, 200 μl of the isolated exosomes were incubated with 5-8 μl/1 ml of the dye for 1 h at RT, then added to 4 ml of filtered 1X PBS, ultracentrifuged at 110,000 x g for 1.5 h at 4˚C, and resuspended in 700 μl of filtered 1X PBS. The medium of MCF7 or A549 or fibroblasts cells (all at $1.5x10^5$ cells per well) was then replaced with serum-free medium (SFM) containing 50 μg/ml of iMSC-Exos or BMSC-Exos. After 16 h of treatment, the cells were washed with 1X PBS and incubated for an additional 16 h. Subsequently, the cells were incubated for 30 min at RT with 5-chloromethylfluorescein diacetate dye (CMFDA; Invitrogen; Thermo Fisher Scientific, Inc.), fixed with 4% PFA, incubated for 15 min at RT, washed with 1X PBS, and stained for 5 min at RT with 4',6-diamidino-2-phenylindole (DAPI; Invitrogen; Thermo Fisher Scientific, Inc.). Finally, the cells were mounted with mounting medium (Abcam). The cellular internalization of iMSC-Exos or BMSC-Exos was observed under a time-lapse microscope (Carl Zeiss).

Cell proliferation assay. MCF7, A549 and fibroblast cells ($8x10^3$ cells per well) were cultured in 96-well plates with 100 μl of RPMI-1640 medium for 24 h at 37˚C and 5% CO_2. Following this initial incubation, the medium was replaced with serum-free RPMI-1640 containing 350 μl of either iMSC-Exos or BMSC-Exos (50 μg/ml). Cell proliferation was measured after 24, 48, and 72 h by adding 10 μl of thiazolyl blue tetrazolium bromide reagent (MTT; Promega) to each well, followed by a 3-h incubation at 37˚C. Subsequently, 100 μl of solubilization stop solution (Promega Corporation) was added, and the plates were incubated for an additional 30 min at 37˚C. The absorbance of the cells was then measured at 570 nm using a BioTek microplate reader (5), and the data were analyzed with BioTek Gen 5 data analysis software (BioTek; Agilent Technologies, Inc.).

Apoptosis analysis. Cell apoptosis was assessed using the eBioscience™ Annexin V-FITC Apoptosis Detection Kit (cat. no. 88-8005-74; Invitrogen; Thermo Fisher Scientific, Inc.) and analyzed by flow cytometry. Briefly, A549 and MCF7 cell lines were seeded at a density of $3x10^5$ cells per well and treated with or without 50 μg/ml of iMSC-Exos or BMSC-Exos for 48 h after replacing the medium with serum-free RPMI-1640. Following treatment, cells were collected and washed with 1X PBS. The cell pellet was then resuspended in 100 μl of 1X Binding Buffer, mixed with 5 μl of FITC-conjugated Annexin V and incubated in the dark at RT for 15 min. Subsequently, 5 μl of propidium iodide (PI) was added to each sample, followed by 100 μl of 1X Binding Buffer to dilute the cell suspension. The samples were then analyzed using a BD FACSCanto II flow cytometer and BD FACSDiva software.

Scratch wound assay. MCF7 or A549 cells were seeded at a density of $3x10^5$ cells per well. Upon reaching 90% confluency, an artificial wound was created by scratching the cell monolayer with a 200-μl pipette tip. The medium was then changed to serum-free RPMI-1640, and the cells were washed twice with 1X PBS before being treated with 50 μg/ml of iMSC-Exos or BMSC-Exos. Images were recorded using EVOS XL Core Imaging System (Thermo Fisher Scientific, Inc.), at 0, 9, 20, and 47 h after treatment and the distance of cell migration was measured using ImageJ software (version 1.53; National Institutes of Health) (5).

Senescence assay. Senescence-associated β-galactosidase (SA-βGal) staining was performed on treated cells using a senescence detection kit (cat. no. ab65351; Abcam). Briefly, MCF7 or A549 cells were seeded at a density of $3x10^5$ cells per well in RPMI-1640 medium. The following day, the medium was replaced with serum-free RPMI-1640 containing 50 μg/ml of either iMSC-Exos or BMSC-Exos. After 48 h, the medium was aspirated, and the cells were washed once with 1 ml of 1X PBS and fixed with 0.5 ml of fixative solution provided in the kit for 15 min at RT. Subsequently, 0.5 ml of staining solution, prepared by mixing 5 μl of 100X staining supplement, and 25 μl of 20 mg/ml X-Gal in dimethylsulfoxide with 470 μl of staining solution (all included in the aforementioned kit), was added, and the cells were incubated at 37˚C for 12 h. The cells were then observed under a microscope (EVOS XL Core Imaging System; Thermo Fisher Scientific, Inc.) to investigate the development of blue color, which indicates senescence, and were manually counted and compared to untreated cells.

Statistical analysis. All data were analyzed using GraphPad Prism version 9.1.0 (Dotmatics). The statistical tests included an unpaired Student's t-test or a two-way analysis of variance (ANOVA), followed by a Bonferroni post-hoc test when indicated. Data are presented as the mean ± standard error (SE), and a $P \leq 0.05$ was considered to indicate a statistically significant difference. All the experiments were conducted in three independent replicates (n=3).

Results

Characterization of iMSC and BMSC surface markers by flow cytometry. A flow cytometric analysis was initially performed to detect the expression of stem cell surface markers on iMSCs and BMSCs. The analysis clearly revealed the expression of CD105, CD90, CD73, and CD44 on both iMSCs and BMSCs (Fig. 1A), with negative expression of CD34, CD11b, CD19, CD45, and HLA-DR surface markers. The expression percentages of the aforementioned markers in the BMSCs were as follows: CD105 was expressed in 97% of the cells, CD90 was expressed in 98.6%, CD73 was expressed in 99%, and CD44 was expressed in 98.7% (Fig. 1B). In comparison, the average expression percentages for iMSCs were 91% for CD105, 98.3% for CD90, 99% for CD73, and 99% for CD44 (Fig. 1B). Additionally, both iMSCs and BMSCs were tested for their ability to differentiate into osteogenic (Fig. 1C) and

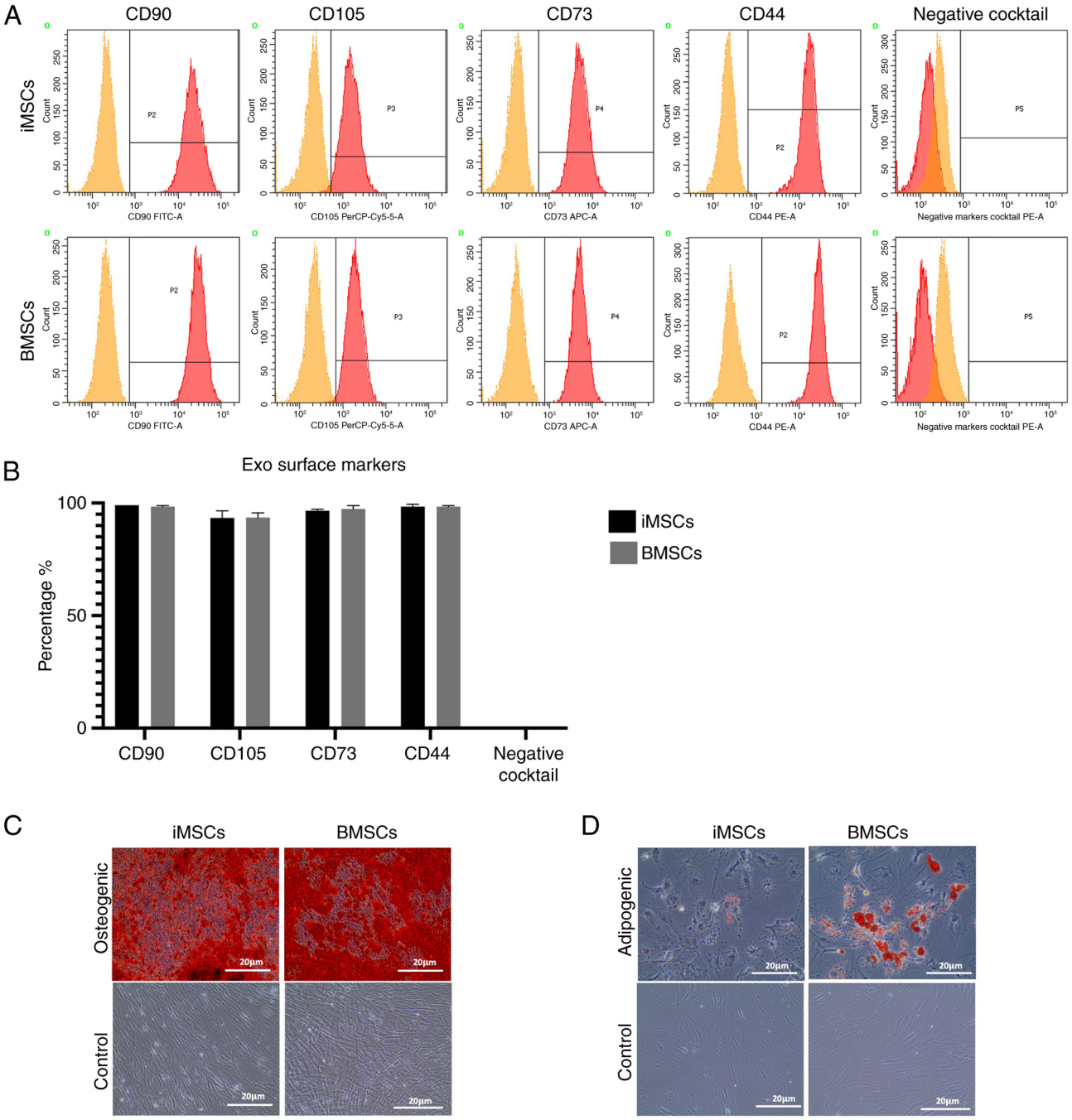

Figure 1. Analysis of surface markers and differentiation potential of iMSCs and BMSCs. (A) Histograms of flow cytometric analysis of iMSCs and BMSCs. (B) Bar graphs of percentages of MSCs surface markers (CD90, CD105, CD73 and CD44) in iMSCs and BMSCs. (C) Osteogenic differentiation potential of iMSCs and BMSCs. (D) Adipogenic differentiation potential of iMSCs and BMSCs. iMSCs, induced pluripotent stem cell-derived mesenchymal stem cells; BMSCs, bone marrow stromal mesenchymal stem cells; Exo, exosome.

adipogenic (Fig. 1D) lineages. The results obtained from the present study revealed the positive differentiation potential of both cell types, with BMSCs showing higher levels of adipogenic differentiation than iMSCs.

Characterization of isolated BMSC-Exos and iMSC-Exos. The exosomes were bound to sulfate-latex beads to detect exosome surface markers using flow cytometry (CD81, CD9, and CD63), as aforementioned. The analysis confirmed the successful expression of these markers in both the iMSC-Exos and the BMSC-Exos. Notably, both types of exosomes presented higher expression levels of the CD9 tetraspanin protein than CD81 and CD63. However, no significant differences in the expression of exosome surface markers were observed between the two groups (Fig. 2A and B). The average percentages of these markers in iMSC-Exos were as follows: CD9 (99%), CD81 (79%), and CD63 (64%). In comparison, BMSC-Exos exhibited average percentages of CD9 of 95%, CD81 of 77%, and CD63 of 40% (Fig. 2A and B). The size distribution analysis revealed that both iMSC- and BMSC-derived exosomes exhibited heterogeneous size ranges of 88-220 nm and 32-117 nm, respectively, with iMSC-Exos

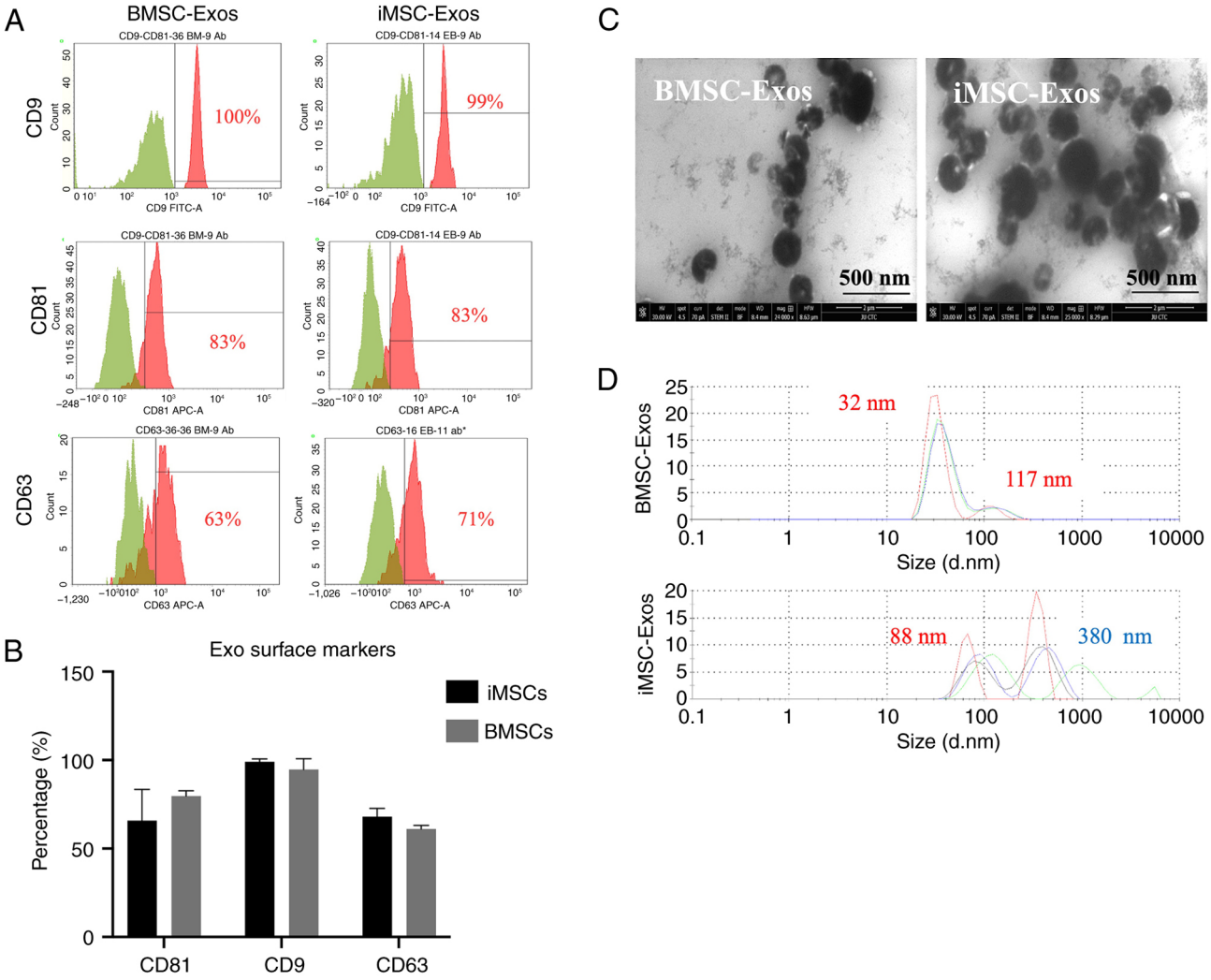

Figure 2. Characterization of isolated BMSC-Exos and iMSC-Exos. (A) Representative histograms of flow cytometric analysis of exosome surface markers (CD9, CD81 and CD63) in iMSC-Exos and BMSC-Exos. (B) Graph bar of percentages of surface markers present in iMSC-Exos and BMSC-Exos. (C) Representative transmission electron microscopy images of iMSC-Exos and BMSC-Exos; scale bar, 500 nm. (D) Dynamic light scattering analysis based on the isolated size intensity distribution of exosomes. BMSCs, bone marrow stromal mesenchymal stem cells; Exos, exosomes; iMSCs, induced pluripotent stem cell-derived mesenchymal stem cells.

having a larger average size than BMSC-Exos (Fig. 2D). TEM revealed a typical cup-like shape of both iMSC-Exos and BMSC-Exos (Fig. 2C). Additionally, the aggregates observed for the iMSC-Exos were consistent with the DLS findings, which indicated a larger average size for the iMSC-Exos than for the BMSC-Exos. Overall, the characteristics of the isolated EVs were consistent with those of the exosomes.

Internalization of iMSC- and BMSC-derived exosomes. Subsequently, the uptake efficiency of exosomes by two cancer cell lines was assessed (namely, MCF7 and A549, as well as nonmalignant fibroblasts) by incubating them with either iMSC-derived or BMSC-derived exosomes for 12 h. The exosomes were prelabeled with DiI-O, a lipophilic red-orange, fluorescent dye. The cells were also stained with CMFDA (green) to visualize the cytoplasm, and DAPI (blue) was used for nuclear staining. After 12 h of incubation with DiI-O-labeled exosomes, the cells were fixed and examined under a fluorescence microscope. Imaging data confirmed the successful internalization of iMSC-Exos and BMSC-Exos into MCF7 (Fig. 3A) and A549 cells (Fig. 3B), as well as nonmalignant fibroblasts (Fig. S1).

Transient suppression of the proliferation of MCF7 cells is observed with both exosome types, whereas the proliferation of A549 cells is suppressed by iMSC-Exos. The effects of both exosome types on cancer cell proliferation and survival were examined. Cancer cell proliferation was assessed using an MTT assay to evaluate the effects of iMSC-Exos and BMSC-Exos at 24 and 48 h of treatment. Compared to untreated SFM cells, both MCF7 and A549 cells showed a significant suppression of proliferation after 24 h of treatment with either type of exosome ($P \leq 0.0001$ for both) (Fig. 4A and B). Moreover, BMSC-Exos had a greater inhibitory effect than iMSC-Exos on MCF7 cells at 24 h after treatment ($P \leq 0.01$).

Notably, the significant antitumor effect observed at 24 h compared with that of SFM did not persist at 48 h in MCF7 cells treated with both types of exosomes or in A549 cells treated with BMSC-Exos, indicating a transient effect of BMSC-Exos on MCF7 and A549 cells and of iMSC-Exos on

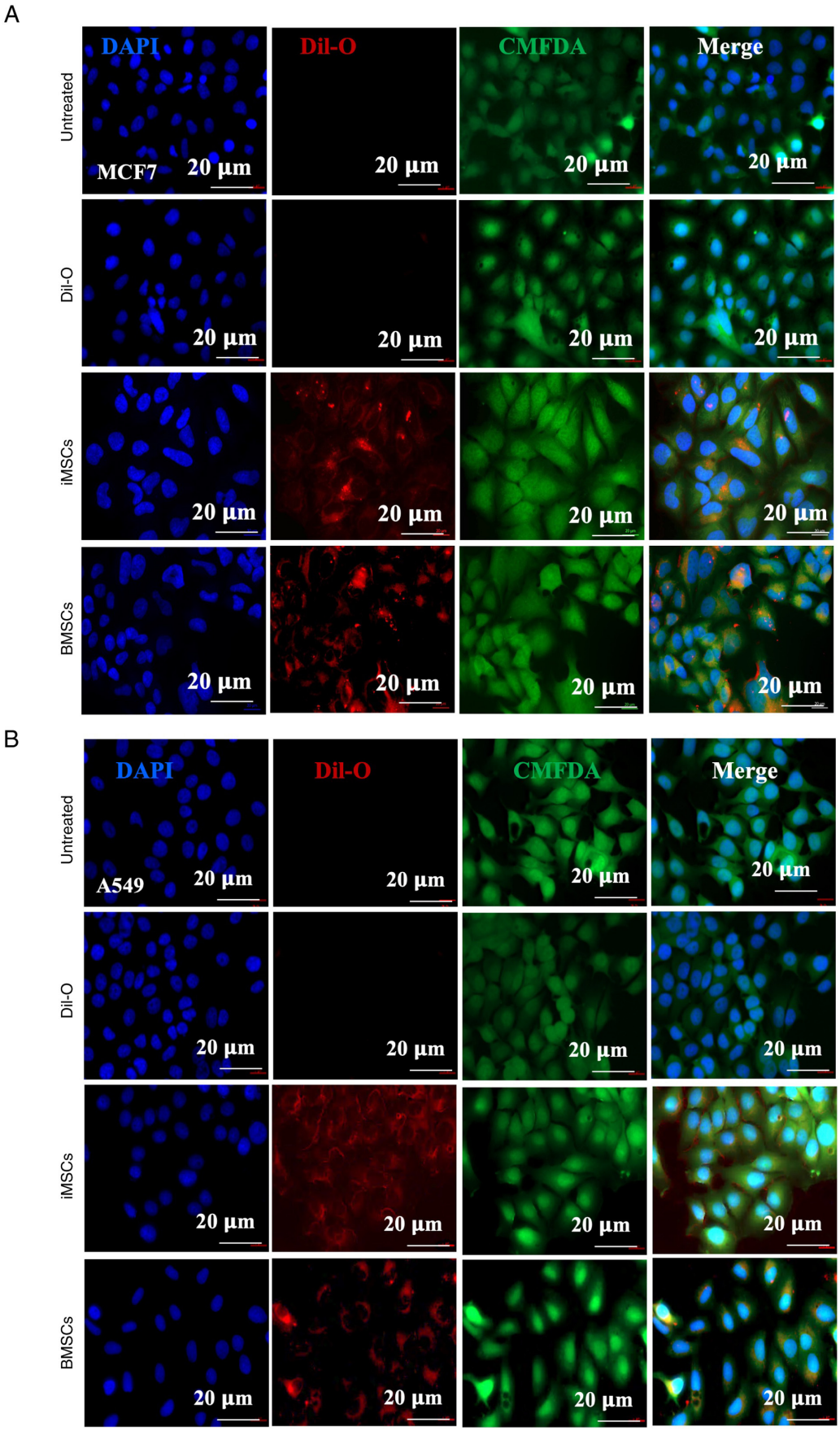

Figure 3. Assessment of the internalization of iMSC-Exos and BMSC-Exos into cancer cells. (A) MCF7 and (B) A549 cells were either left untreated (first panel), incubated with DiI-O dye only (second panel), or incubated with DiI-O-labeled exosomes from iMSCs (third panel) and BMSCs (fourth panel). DAPI staining was used to visualize the nuclei and CMFDA to stain the cell bodies. Scale bar, 20 μm. (n=3). iMSCs, induced pluripotent stem cell-derived mesenchymal stem cells; Exos, exosomes; BMSCs, bone marrow stromal mesenchymal stem cells; DiI-O, 1,1'-dioctadecyl-3,3,3',3'-tetramethylindocarbocyanine perchlorate; CMFDA, 5-chloromethylfluorescein diacetate dye; DAPI, 4',6-diamidino-2-phenylindole.

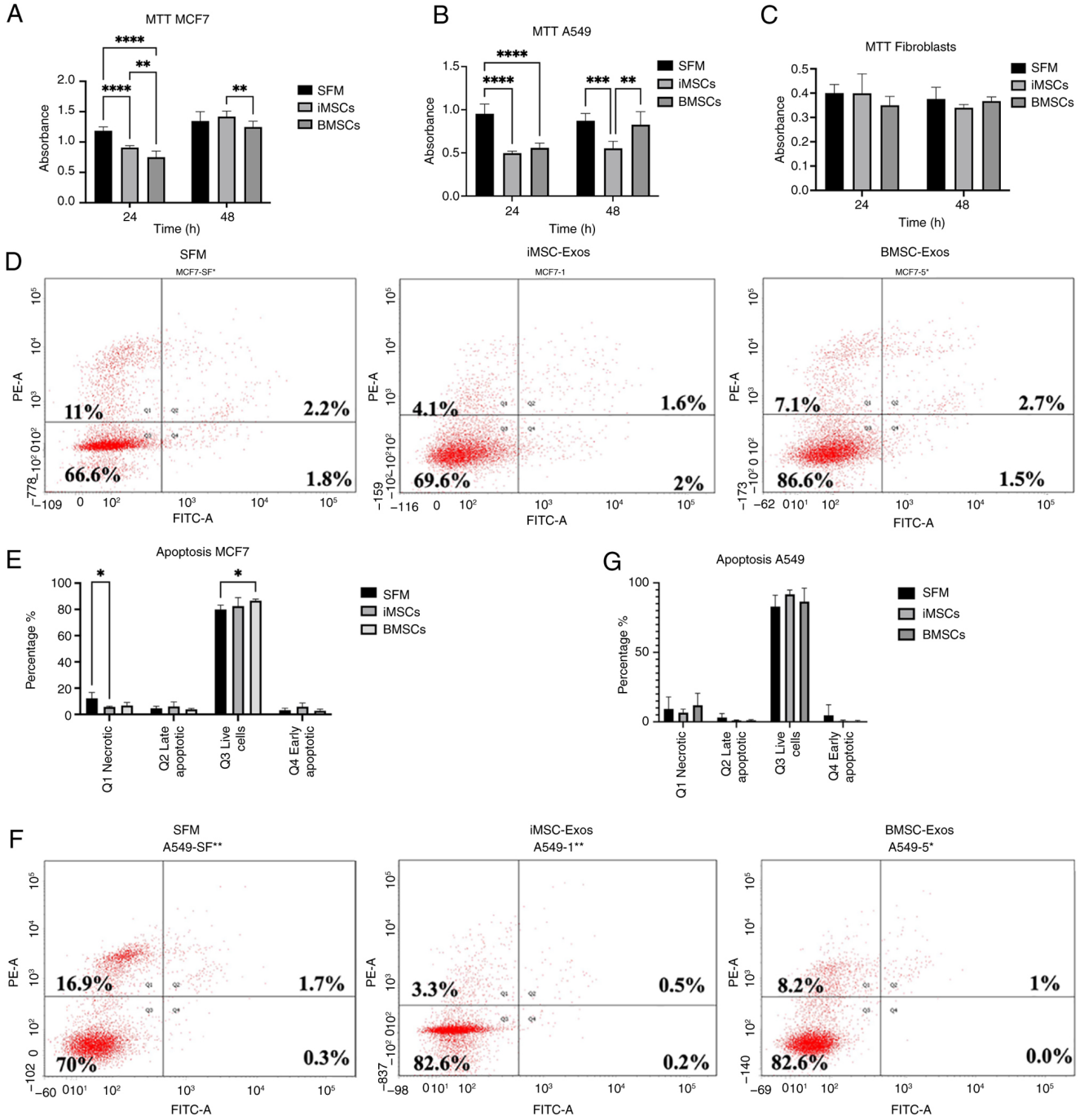

Figure 4. Assessment of proliferation and apoptosis on treated MCF7 and A549 cells with iMSC-Exos or BMSC-Exos. An MTT assay was used to assess the proliferation of (A) MCF7, (B) A549, and (C) fibroblasts following 24 and 48 h of incubation with iMSC-Exos, BMSC-Exos, or SFM. Representative FACS plot images of (D) MCF7 and (F) A549 cells. (E) Apoptosis assay results for treated MCF7 cells, showing Q1 (necrotic cells), Q2 (late apoptotic cells), Q3 (live cells), and Q4 (early apoptotic cells). (G) Apoptosis assay results for treated A549 cells. Data are presented as the mean ± SE; (n=3). *P≤0.05, **P≤0.01 ***P≤0.001, ****P≤0.0001. iMSCs, induced pluripotent stem cell-derived mesenchymal stem cells; Exos, exosomes; BMSCs, bone marrow stromal mesenchymal stem cells; SFM, serum-free medium; FACS, fluorescence-activated cell sorting; SE, standard error.

MCF7 cells. However, within 48 h of treating the MCF7 cells with the BMSC-Exos, cell proliferation decreased compared with that of the MCF7 cells treated with the iMSC-Exos (P≤0.01). In A549 cells, the suppressive effect of iMSC-Exos persisted over time, as evidenced by a continued reduction in proliferation at 48 h compared with that of the SFM control (P≤0.001) and BMSC-Exos (P≤0.01). Additionally, the treatment of fibroblasts that were used as control cells with either type of exosome had no significant effect on proliferation (Fig. 4C). The findings of the present study suggested that the antiproliferative effect may be cancer-specific.

Next, the effect of the BMSC-Exos and iMSC-Exos on the induction of apoptosis in the MCF7 and A549 cells was assessed using flow cytometry of the Annexin V/PI-stained cells. Treatment of MCF7 cells with either iMSC-Exos or BMSC-Exos for 48 h resulted in no significant increase in the number of early apoptotic cells (Annexin V^{+}/PI^{-}) or late apoptotic cells (Annexin V^{+}/PI^{+}) (Fig. 4E). Similarly, no significant

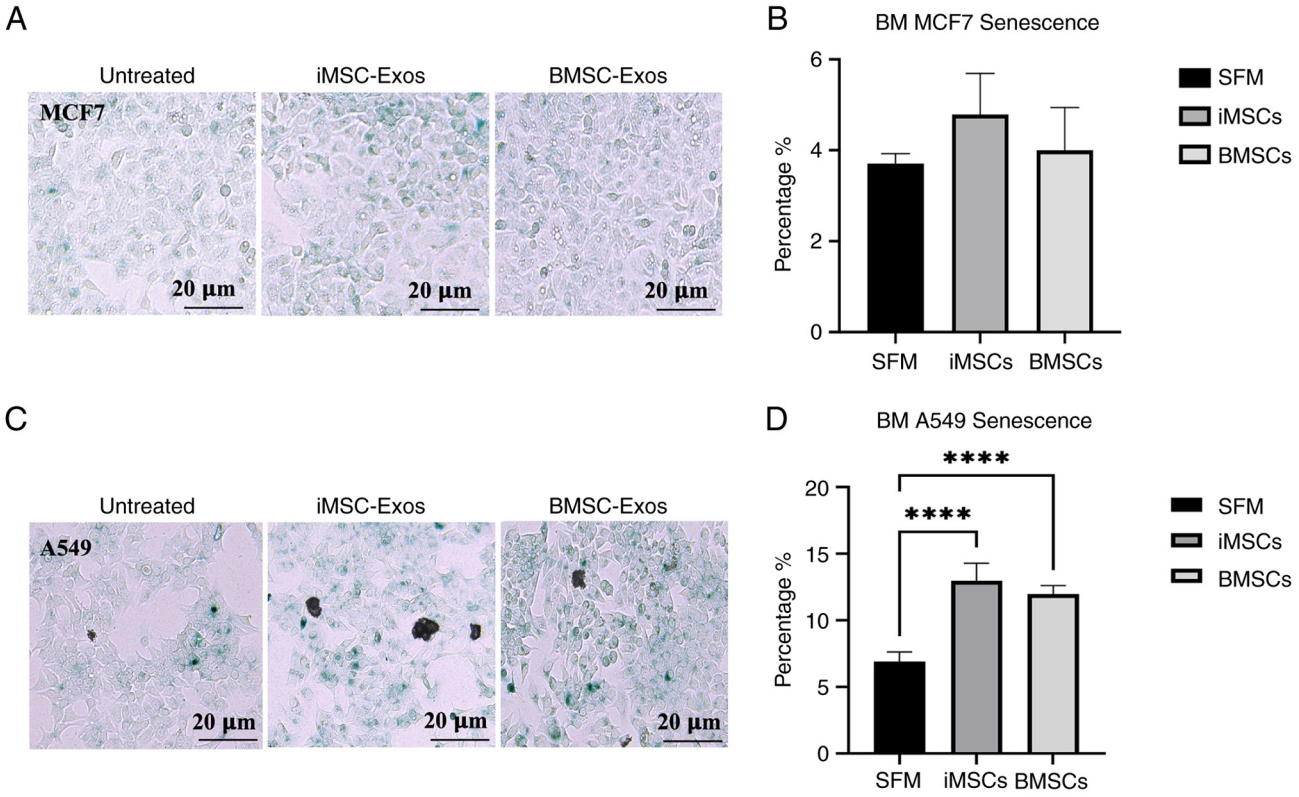

Figure 5. Analysis of SA-βGal-positive cancer cells. Representative images and relative quantification of SA-βGal-positive cells of (A and B) MCF7 and (C and D) A549 cells after 48 h of treatment with iMSC-Exos or BMSC-Exos. Scale bar, 200 μm. Data are presented as the mean ± SE; (n=3). ****P≤0.0001. SA-βGal, senescence-associated β-galactosidase; iMSCs, induced pluripotent stem cell-derived mesenchymal stem cells; BMSCs, bone marrow stromal mesenchymal stem cells; SFM, serum-free medium; SE, standard error; BM, bone marrow.

differences in apoptosis were observed in A549 cells treated with either BMSC-Exos or iMSC-Exos (Fig. 4G).

Significant increase in the number of SA-βGal-positive A549 cells after treatment. The percentage of cells positive for SA-βGal activity, which reflects cellular senescence, was determined by counting the number of blue cells in the total population, as described by Debacq-Chainiaux *et al* (58). In MCF7 cells treated with iMSC-Exos or BMSC-Exos, the percentage of SA-βGal-positive cells was not significantly different (Fig. 5A and B). The findings of the present study indicated that no significant induction of cellular senescence occurred in MCF7 cells treated with either type of exosome. By contrast, treatment of A549 cells with either BMSC-Exos or iMSC-Exos resulted in a significant increase in senescence compared with that of the control (both P<0.0001) (Fig. 5C and D). These results indicate that the effect of exosome treatment on cellular senescence in tumor cells may be minimal.

Time-dependent effects of iMSC- and BMSC-derived exosomes on migration. A scratch wound healing assay was performed to assess the effects of iMSC- and BMSC-derived exosomes on MCF7 and A549 cancer cells. A scratch was made through the monolayers of cancer cells, and microscopy images of the scratch wounds were captured at ~9, 20, and 47 h after treatment with iMSC- or BMSC-derived exosomes. In MCF7 cells treated with BMSC-derived exosomes, a significant increase in migration was observed at ~20 h (P≤0.01) (Fig. 6A and B). However, this effect was reversed at ~47 h (P≤0.05), indicating a time-dependent effect of the BMSC-Exos on these cells. By contrast, no significant difference in migration was observed in A549 cells treated with either type of exosomes compared with the SFM control (Fig. 6C and D).

Discussion

iPSCs represent a promising alternative to traditional MSC sources, potentially overcoming the challenges associated with limited expandability and source variability (16). BMSC-derived exosomes have demonstrated significant therapeutic potential in various bone diseases and are gaining recognition for their broader applications in regenerative medicine, particularly in orthopedic conditions (59). For example, they protect against cartilage damage and alleviate knee pain in osteoarthritis models (60) and promote chondrocyte proliferation to mitigate osteoarthritis (61). The relationship between MSC-derived exosomes and cancer remains ambiguous, as studies have reported conflicting results regarding the effects of MSC-derived EVs on cancer (62,63). These conflicting results may be attributed to variations in the origin of MSCs, the methods used for isolating MSCs (64), or the specific types of tumor models employed in the studies (64,65). However, the therapeutic potential of iPSC-derived MSCs and their exosomes requires further investigation to fully understand their impacts on cancer. The present study provided insights into the comparative effects of exosomes derived from iMSCs and BMSCs on

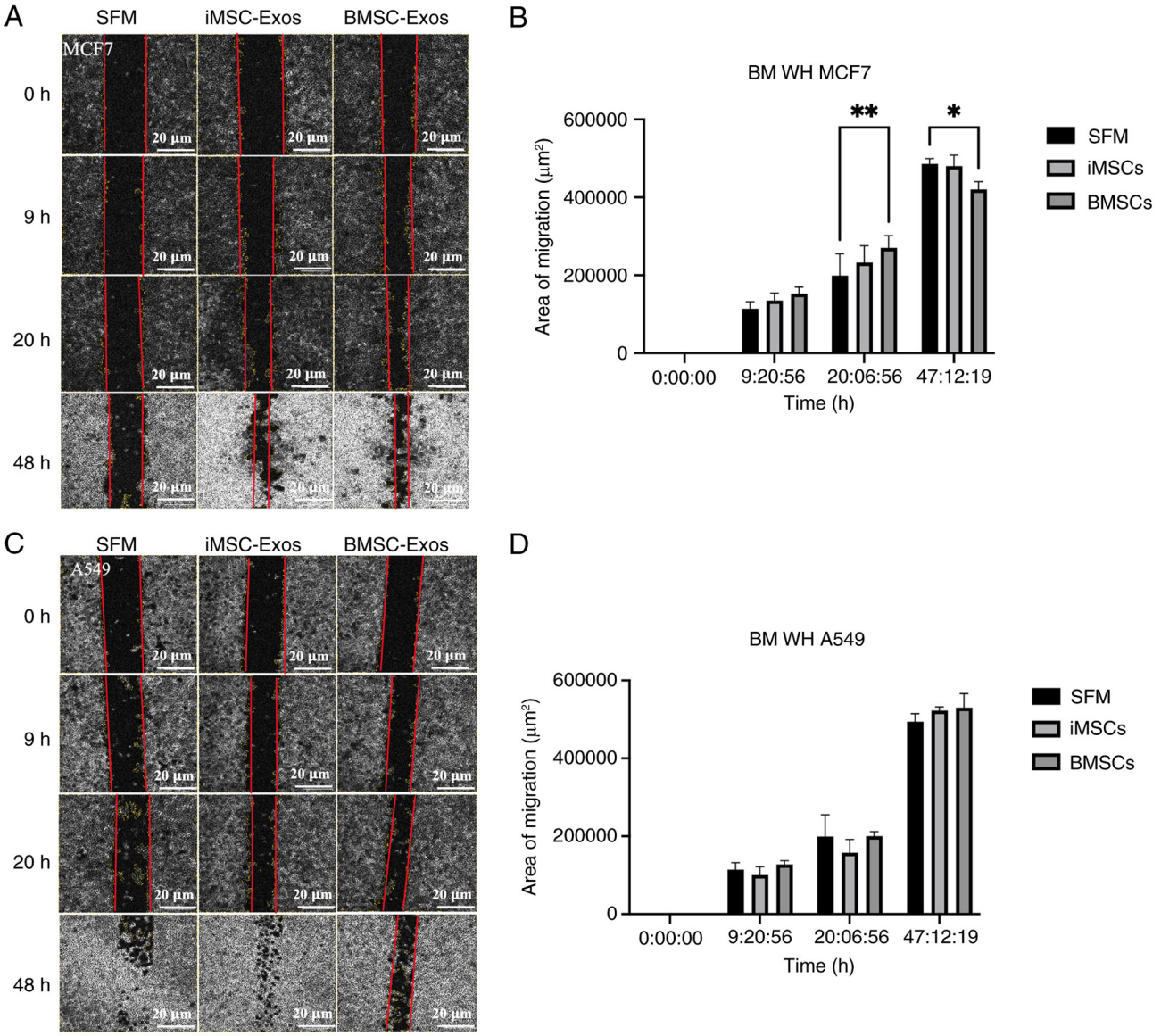

Figure 6. Time-dependent migration effects of iMSC- and BMSC-derived exosomes on MCF7 and A549 cancer cells. (A) Representative microscopy images of the scratch in the MCF7 cell monolayer at different time points following treatment with either iMSC- or BMSC-derived exosomes. (B) The area of the scratch that was covered by migrating cells was measured using ImageJ and presented as the area of migration at different time points. (C and D) Representative microscopy images of the scratch in the A549 cell monolayer, and the quantification of the area of migration, respectively. Data are represented as the mean ± SE; (n=3). Significance levels are indicated as follows: $^{*}P\leq0.05$ and $^{**}P\leq0.01$. iMSCs, induced pluripotent stem cell-derived mesenchymal stem cells; BMSCs, bone marrow stromal mesenchymal stem cells; SE, standard error; BM, bone marrow; WH wound healing.

cancer cells, contributing to ongoing research efforts aimed at elucidating their roles in cancer biology.

In the present study, both iMSCs and BMSCs were successfully characterized according to the ISCT criteria (66). These cells exhibited positive expression of stem cell surface markers (CD90, CD105, CD73, and CD44), a spindle-like morphology, adherence to plastic, and the ability to differentiate into osteogenic and adipogenic lineages *in vitro*. Previous research, such as work by Maleki *et al* (67), has reported that the expression of MSC surface markers can vary significantly depending on the source of the MSCs. In their study, four types of MSCs [spermatogonial stem cells (SSCs), hair follicle stem cells, granulosa cells, and WJ-MSCs], were analyzed. SSCs showed the highest expression of CD44, which is associated with maintaining stemness, CD90, that is linked to growth and differentiation, and CD105, which plays a role in osteogenesis. However, despite these potential differences, both the BMSCs and iMSCs in the present study exhibited high expression levels of classical hMSC markers (>90%). Exosomes were isolated through the sequential centrifugation and filtration of CM, followed by ultracentrifugation. These exosomes were characterized using flow cytometry to detect exosome surface markers from the tetraspanin family, including CD9, CD81, and CD63 (68). Both groups of exosomes expressed these markers, with a higher percentage of CD9 expression observed in each set. Notably, CD9 is associated with modulating cell adhesion and migration in breast cancer-derived EVs, suggesting a potential role in cancer metastasis (69).

Further analysis of the isolated exosomes revealed a size distribution of 32-117 nm for the BMSC-Exos and 88-220 nm for the iMSC-Exos. An additional reading with an average

size of 380 nm, which appeared to have a lower intensity in the size distribution measurement of iMSC-Exos, likely resulted from the presence of iMSC-Exo aggregates. This aggregation was confirmed via TEM when morphology was studied. Aggregation is a primary limitation of collecting exosomes following sequential ultracentrifugation; however, it remains an effective method for collecting sufficient exosomes from large volumes of conditioned media (70). To minimize aggregation, several exosome isolation methods can be used. Exosome precipitation kits that utilize reagents such as PEG to precipitate exosomes from the sample are one option (71). Magnetic bead-based isolation, using magnetic beads coated with antibodies targeting specific exosome surface markers (for example CD9 and CD63), selectively captures exosomes, providing high specificity and avoiding aggregation that can occur with ultracentrifugation (72). Polymer-based precipitation (for example ExoQuick) can also be used to precipitate exosomes from biological fluids, offering a simpler and quicker alternative to ultracentrifugation (73,74). While these alternative methods can help reduce aggregation, ultracentrifugation remains a widely employed, cost-effective, and scalable technique, making it well-suited for the requirements the present study. However, despite the heterogeneity in size, iMSC-Exos were generally larger. Given that the typical size range of exosomes is 30-150 nm (35,75), both sets of isolated exosomes generally fell within this range.

The results of the proliferation assay using MCF7 and A549 cells revealed that both iMSC-Exos and BMSC-Exos significantly decreased cell proliferation at 24 h, with no significant decrease in MCF7 cell proliferation observed at 48 h after treatment with iMSC-Exos. However, A549 cells were significantly affected after 48 h of treatment with iMSC-Exos. In fact, iMSC-Exos resulted in greater proliferation at 48 h than did BMSC-Exos. The findings of the present study suggested that while the exosomes initially inhibited MCF7 cell proliferation, their effects may have diminished over time. By contrast, for A549 cells, iMSC-Exos had a greater inhibitory effect on proliferation at 48 h than did BMSC-Exos. The finding of the present study aligned with that of previous research documenting the effects of human stem cells on reducing the proliferation of the A549 cell line (76). However, the proliferation rate of MCF7 cells was not significantly different from that of cells cultured in SFM at 48 h after treatment with either iMSC-Exos or BMSC-Exos, despite the initial antitumor effect observed at 24 h. Additionally, a decrease in necrosis was observed in cells treated with iMSC-Exos compared with those treated with SFM. The findings of the present study suggested a potential suppressive effect of BMSC-Exos on MCF7 cells at 48 h, which may have contributed to the diminished antitumor effect observed at 24 h in the proliferation assay, possibly due to the increased number of viable cells at the later time points.

Overall, these observations are consistent with previous studies that reported variability in the impact of MSC-derived exosomes on cancer cell proliferation, which is often influenced by the source of the MSCs (64) and the specific cancer model used (64,74). Previous studies revealed that BMSC-Exos can exert either pro- or anti-tumor effects depending on their molecular content and target pathways. Wu *et al* (77) reported that BMSC-Exos carrying miR-30b-5p suppressed non-small cell lung cancer proliferation by targeting EZH2 and other genes involved in the PI3K/AKT signaling pathway, while Wang *et al* (44) found that BMSC-Exos promote lung cancer progression, as shown in the A549 cell model through miR-425-mediated suppression of CPEB1. These findings suggest that the cargo composition of exosomes plays a crucial role in determining their effects on proliferation. Similarly, in breast cancer, Chen *et al* (78) showed that BMSC-Exos promote breast cancer proliferation in the MCF7 model by activating the Hedgehog signaling pathway, whereas Hu *et al* (79) demonstrated that BMSC-Exos carrying AlkB homolog 5 (ALKBH5) suppress triple-negative breast cancer cell growth by regulating the ALKBH5-dependent mechanism, involving the UBE2C gene and p53 regulation. Further studies are needed to determine the molecular pathways responsible for the differential and time-dependent impact of BMSC-Exos and iMSC-Exos on cancer cell proliferation. However, although the MTT assay has been widely employed to measure cell viability, it is worth emphasizing, according to Liu *et al* (80), that utilizing alternative assays, such as WST-based methods (for example CCK-8), could address the limitations of MTT and enhance the reliability and efficiency of viability analyses. The MTT assay relies on mitochondrial enzymes to reduce MTT into insoluble formazan crystals, but it has limitations including toxicity and the need for solubilization. By contrast, WST assays, such as CCK-8, use water-soluble tetrazolium salts reduced by dehydrogenases into soluble formazan, offering advantages such as non-toxicity, no solubilization, and improved enzymatic detection, which could make them a better alternative to MTT, as discussed by Liu *et al* (80).

Although no significant migration of A549 cells was observed following exosome treatment, compared with SFM, BMSC-derived exosomes increased the migration of MCF7 cells at 20 h. Notably, this effect was reversed at 47 h, with increased migration observed in the serum-free condition. This behavior suggests a dynamic interaction between exosomes and the cell migration process over time or potentially due to the experimental conditions. Considering the original hypothesis that increased proliferation rates are associated with increased migration rates, the findings of the present study indicated that the relationship between exosome treatment and cell behavior may be more complex. Further investigation is needed to understand the underlying mechanisms driving these time-dependent changes in migration (81,82). The findings of the present study from MCF7 cells contradict the theory that increased proliferation is associated with increased migration. Instead, they are consistent with other studies suggesting that proliferation and migration can be contrasting events (82-84). Notably, both the proliferation and migration assays revealed a time-dependent effect on MCF7 cells treated with BMSC-Exos. A significant antitumor effect was observed in the proliferation assay at 24 h, whereas the migration assay showed the opposite effect at 47 h compared with 20 h, indicating complex and dynamic cellular responses to exosome treatment over time.

The quantification of SA-βGal-positive cells via a senescence assay revealed an increase in the senescence of both A549 and MCF7 cells following treatment with iMSC-Exos and BMSC-Exos, with only A549 cells showing a statistically significant effect. Cellular senescence is characterized by irreversible cell cycle arrest, leading to the inhibition of

proliferation, thus highlighting its role as a tumor-suppressive mechanism (85). This increase in senescence aligns with the decreased proliferation of A549 cells observed in the MTT assay, suggesting that the antitumor effects of iMSC-Exos and BMSC-Exos on A549 cells are mediated, at least in part, by the induction of senescence. The finding of the present study is consistent with previous studies highlighting the tumor-suppressive role of senescence in cancer (25,86,87). By contrast, the absence of a significant effect on MCF7 cells may reflect differences in cell type-specific responses to exosome treatment, potentially due to variations in the molecular pathways regulating proliferation and senescence. The increased senescence observed in A549 cells treated with iMSC-Exos compared with BMSC-Exos could be attributed to differences in their molecular cargo, such as increased levels of senescence-inducing microRNAs, proteins, or epigenetic regulators (85).

It is suggested that future studies use patient-derived xenograft models and larger cohorts to confirm these findings and ensure broader applicability. For example, Yaghoubi *et al* (88) reported that the overexpression of miR-145-5p in human umbilical MSC-derived exosomes reduced xenograft tumor growth, highlighting the potential of exosomes in cancer treatment. In conclusion, the present study described the distinct effects of exosomes derived from BMSCs and iMSCs on MCF7 and A549 cancer cells, highlighting the variability in cellular responses to exosome treatment. Both types of exosomes exerted potential antitumor effects. These findings underscore the importance of further research to enhance our understanding and optimize the therapeutic use of MSC-derived exosomes in cancer treatment.

Acknowledgements

The authors would like to thank Professor Hatem Al-Kateib from the University of Jordan/Faculty of Pharmacy for helping with the DLS measurement and Miss Rola Bqaien at the Cell Therapy Center/University of Jordan for her assistance in TEM imaging of purified EVs.

Funding

No funding was received.

Availability of data and materials

The data generated in the present study may be requested from the corresponding author.

Authors' contributions

NAA performed the formal analysis, designed the methodology, validated the data, wrote, reviewed, and edited the manuscript as well as supervised the project. RA wrote the original draft and contributed to data acquisition and analysis. SN designed the methodology, performed the formal analysis, validated the data and contributed to writing the original draft. MAI designed the methodology and performed formal analysis. RB, SAH, AAl and FKA validated the methodological procedures and contributed to data acquisition. AHAH and TS wrote, reviewed and edited the manuscript and contributed to data analysis and interpretation. AAw provided the resources, and conceptually designed the project. NAA and AAw confirm the authenticity of all the raw data generated as part of this work. All authors read and approved the final manuscript.

Ethics approval and consent to participate

The present study was reviewed and approved (approval no. IRB/7/2019) by the Ethics Committee Institutional Review Board of the Cell Therapy Center/University of Jordan (Amman, Jordan). All participants provided written informed consent to participate in the present study.

Patient consent for publication

Not applicable.

Competing interests

The authors declare that they have no competing interests.

References

1. Siegel RL, Giaquinto AN and Jemal A: Cancer statistics, 2024. CA Cancer J Clin 74: 12-49, 2024.
2. Sonkin D, Thomas A and Teicher BA: Cancer treatments: Past, present, and future. Cancer Genet 286-287: 18-24, 2024.
3. Hoang DM, Pham PT, Bach TQ, Ngo ATL, Nguyen QT, Phan TTK, Nguyen GH, Le PTT, Hoang VT, Forsyth NR, *et al*: Stem cell-based therapy for human diseases. Signal Transduct Target Ther 7: 272, 2022.
4. Fus-Kujawa A, Mendrek B, Trybus A, Bajdak-Rusinek K, Stepien KL and Sieron AL: Potential of induced pluripotent stem cells for use in gene therapy: History, molecular bases, and medical perspectives. Biomolecules 11: 699, 2021.
5. Shojaei S, Hashemi SM, Ghanbarian H, Salehi M and Mohammadi-Yeganeh S: Effect of mesenchymal stem cells-derived exosomes on tumor microenvironment: Tumor progression versus tumor suppression. J Cell Physiol 234: 3394-3409, 2019.
6. Li X, Peng B, Zhu X, Wang P, Xiong Y, Liu H, Sun K, Wang H, Ou L, Wu Z, *et al*: Changes in related circular RNAs following ERβ knockdown and the relationship to rBMSC osteogenesis. Biochem Biophys Res Commun 493: 100-107, 2017.
7. Fu X, Liu G, Halim A, Ju Y, Luo Q and Song AG: Mesenchymal stem cell migration and tissue repair. Cells 8: 784, 2019.
8. Olmedo-Moreno L, Aguilera Y, Baliña-Sánchez C, Martín-Montalvo A and Capilla-González V: Heterogeneity of in vitro expanded mesenchymal stromal cells and strategies to improve their therapeutic actions. Pharmaceutics 14: 1112, 2022.
9. Vizoso FJ, Eiro N, Cid S, Schneider J and Perez-Fernandez R: Mesenchymal stem cell secretome: Toward cell-free therapeutic strategies in regenerative medicine. Int J Mol Sci 18: 1852, 2017.
10. Wang W and Han ZC: Heterogeneity of human mesenchymal stromal/stem cells. Adv Exp Med Biol 1123: 165-177, 2019.
11. Takahashi K and Yamanaka S: Induction of pluripotent stem cells from mouse embryonic and adult fibroblast cultures by defined factors. Cell 126: 663-676, 2006.
12. Cerneckis J, Cai H and Shi Y: Induced pluripotent stem cells (iPSCs): Molecular mechanisms of induction and applications. Signal Transduct Target Ther 9: 112, 2024.
13. Bindhya S, Sidhanth C, Shabna A, Krishnapriya S, Garg M and Ganesan TS: Induced pluripotent stem cells: A new strategy to model human cancer. Int J Biochem Cell Biol 107: 62-68, 2019.
14. Zhou X, Liu J, Wu F, Mao J, Wang Y, Zhu J, Hong K, Xie H, Li B, Qiu X, *et al*: The application potential of iMSCs and iMSC-EVs in diseases. Front Bioeng Biotechnol 12: 1434465, 2024.
15. Sabapathy V and Kumar S: hiPSC-derived iMSCs: NextGen MSCs as an advanced therapeutically active cell resource for regenerative medicine. J Cell Mol Med 20: 1571-1588, 2016.

16. Wruck W, Graffmann N, Spitzhorn LS and Adjaye J: Human induced pluripotent stem cell-derived mesenchymal stem cells acquire rejuvenation and reduced heterogeneity. Front Cell Dev Biol 9: 717772, 2021.
17. Kopen GC, Prockop DJ and Phinney DG: Marrow stromal cells migrate throughout forebrain and cerebellum, and they differentiate into astrocytes after injection into neonatal mouse brains. Proc Natl Acad Sci USA 96: 10711-10716, 1999.
18. Bittira B, Shum-Tim D, Al-Khaldi A and Chiu RC: Mobilization and homing of bone marrow stromal cells in myocardial infarction. Eur J Cardiothorac Surg 24: 393-398, 2003.
19. Pittenger MF and Martin BJ: Mesenchymal stem cells and their potential as cardiac therapeutics. Cir Res 95: 9-20, 2004.
20. Phinney DG and Pittenger MF: Concise review: MSC-derived exosomes for cell-free therapy. Stem Cells 35: 851-858, 2017.
21. Lin H, Chen H, Zhao X, Chen Z, Zhang P, Tian Y, Wang Y, Ding T, Wang L and Shen Y: Advances in mesenchymal stem cell conditioned medium-mediated periodontal tissue regeneration. J Transl Med 19: 456, 2021.
22. Kumar MA, Baba SK, Sadida HQ, Marzooqi SA, Jerobin J, Altemani FH, Algehainy N, Alanazi MA, Abou-Samra AB, Kumar R, *et al*: Extracellular vesicles as tools and targets in therapy for diseases. Signal Transduct Target Ther 9: 27, 2024.
23. Bogatcheva NV and Coleman ME: Conditioned medium of mesenchymal stromal cells: A new class of therapeutics. Biochemistry (Mosc) 84: 1375-1389, 2019.
24. Cheshomi H and Matin MM: Exosomes and their importance in metastasis, diagnosis, and therapy of colorectal cancer. J Cell Biochem 120: 2671-2686, 2019.
25. Fuloria S, Subramaniyan V, Dahiya R, Dahiya S, Sudhakar K, Kumari U, Sathasivam K, Meenakshi DU, Wu YS, Sekar M, *et al*: Mesenchymal stem cell-derived extracellular vesicles: Regenerative potential and challenges. Biology (Basel) 10: 172, 2021.
26. Brossa A, Fonsato V, Grange C, Tritta S, Tapparo M, Calvetti R, Cedrino M, Fallo S, Gontero P, Camussi G and Bussolati B: Extracellular vesicles from human liver stem cells inhibit renal cancer stem cell-derived tumor growth in vitro and in vivo. Int J Cancer 147: 1694-1706, 2020.
27. Simeone P, Bologna G, Lanuti P, Pierdomenico L, Guagnano MT, Pieragostino D, Del Boccio P, Vergara D, Marchisio M, Miscia S and Mariani-Costantini R: Extracellular vesicles as signaling mediators and disease biomarkers across biological barriers. Int J Mol Sci 21: 2514, 2020.
28. Abels ER and Breakefield XO: Introduction to extracellular vesicles: Biogenesis, RNA cargo selection, content, release, and uptake. Cell Mol Neurobiol 36: 301-312, 2016.
29. Jin Y, Ma L, Zhang W, Yang W, Feng Q and Wang H: Extracellular signals regulate the biogenesis of extracellular vesicles. Biol Res 55: 35, 2022.
30. Vinaiphat A and Sze SK: Advances in extracellular vesicles analysis. Adv Clin Chem 97: 73-116, 2020.
31. Greening DW and Simpson RJ: Understanding extracellular vesicle diversity-current status. Expert Rev Proteomics 15: 887-910, 2018.
32. van Niel G, D'Angelo G and Raposo G: Shedding light on the cell biology of extracellular vesicles. Nat Rev Mol Cell Biol 19: 213-228, 2018.
33. Doyle LM and Wang MZ: Overview of extracellular vesicles, their origin, composition, purpose, and methods for exosome isolation and analysis. Cells 8: 727, 2019.
34. Del Fattore A, Luciano R, Saracino R, Battafarano G, Rizzo C, Pascucci L, Alessandri G, Pessina A, Perrotta A, Fierabracci A and Muraca M: Differential effects of extracellular vesicles secreted by mesenchymal stem cells from different sources on glioblastoma cells. Expert Opin Biol Ther 15: 495-504, 2015.
35. Berumen Sánchez G, Bunn KE, Pua HH and Rafat M: Extracellular vesicles: Mediators of intercellular communication in tissue injury and disease. Cell Commun Signal 19: 104, 2021.
36. Skotland T, Sagini K, Sandvig K and Llorente A: An emerging focus on lipids in extracellular vesicles. Adv Drug Deliv Rev 159: 308-321, 2020.
37. Muralikumar M, Manoj Jain S, Ganesan H, Duttaroy AK, Pathak S and Banerjee A: Current understanding of the mesenchymal stem cell-derived exosomes in cancer and aging. Biotechnol Rep (Amst) 31: e00658, 2021.
38. Hu Y, Li X, Zhang Q, Gu Z, Luo Y, Guo J, Wang X, Jing Y, Chen X and Su J: Exosome-guided bone targeted delivery of Antagomir-188 as an anabolic therapy for bone loss. Bioact Mater 6: 2905-2913, 2021.
39. Guo H and Huang X: Engineered exosomes for future gene-editing therapy. Biomater Transl 3: 240-242, 2022.
40. Liu H, Song P, Zhang H, Zhou F, Ji N, Wang M, Zhou G, Han R, Liu X, Weng W, *et al*: Synthetic biology-based bacterial extracellular vesicles displaying BMP-2 and CXCR4 to ameliorate osteoporosis. J Extracell Vesicles 13: e12429, 2024.
41. Zhou Y, Zhou W, Chen X, Wang Q, Li C, Chen Q, Zhang Y, Lu Y, Ding X and Jiang C: Bone marrow mesenchymal stem cells-derived exosomes for penetrating and targeted chemotherapy of pancreatic cancer. Acta Pharm Sin B 10: 1563-1575, 2020.
42. Lin Z, Wu Y, Xu Y, Li G, Li Z and Liu T: Mesenchymal stem cell-derived exosomes in cancer therapy resistance: Recent advances and therapeutic potential. Mol Cancer 21: 179, 2022.
43. Zakiyah N, Wanandi SI, Antarianto RD, Syahrani RA and Arumsari S: Mesenchymal stem cell-derived extracellular vesicles increase human MCF7 breast cancer cell proliferation associated with OCT4 expression and ALDH activity. Asian Pac J Cancer Prev 24: 2781-2789, 2023.
44. Wang G, Ji X, Li P and Wang W: Human bone marrow mesenchymal stem cell-derived exosomes containing microRNA-425 promote migration, invasion and lung metastasis by down-regulating CPEB1. Regen Ther 20: 107-116, 2022.
45. Zhao Q, Hai B, Kelly J, Wu S and Liu F: Extracellular vesicle mimics made from iPS cell-derived mesenchymal stem cells improve the treatment of metastatic prostate cancer. Stem Cell Res Ther 12: 29, 2021.
46. Liu H, Dilger JP and Lin J: Lidocaine suppresses viability and migration of human breast cancer cells: TRPM7 as a target for some breast cancer cell lines. Cancers (Basel) 13: 234, 2021.
47. Li R, Xiao C, Liu H, Huang Y, Dilger JP and Lin J: Effects of local anesthetics on breast cancer cell viability and migration. BMC Cancer 18: 666, 2018.
48. Santucci KL, Snyder KK, Van Buskirk RG, Baust JG and Baust JM: Investigation of lung cancer cell response to cryoablation and adjunctive gemcitabine-based cryo-chemotherapy using the A549 cell line. Biomedicines 12: 1239, 2024.
49. Li J, Zhong X, Zhao Y, Shen J, Xiao Z and Pilapong C: Acacetin inhibited non-small-cell lung cancer (NSCLC) cell growth via upregulating miR-34a in vitro and in vivo. Sci Rep 14: 2348, 2024.
50. Huang PH, Duan XB, Tang ZZ, Zou ZX, Song WM, Gao G, Li D, Nie FQ, Yan X, Fu YX, *et al*: Betulinaldehyde exhibits effective anti-tumor effects in A549 cells by regulating intracellular autophagy. Sci Rep 13: 743, 2023.
51. Ababneh NA, Al-Kurdi B, Jamali F and Awidi A: A comparative study of the capability of MSCs isolated from different human tissue sources to differentiate into neuronal stem cells and dopaminergic-like cells. PeerJ 10: e13003, 2022.
52. Ababneh NA, Al-Kurdi B, Ali D, Abuarqoub D, Barham R, Salah B and Awidi A: Establishment of a human induced pluripotent stem cell (iPSC) line (JUCTCi010-A) from a healthy Jordanian female skin dermal fibroblasts. Stem Cell Res 47: 101891, 2020 (Epub ahead of print).
53. Ababneh NA, Al-Kurdi B, Ali D, Barham R, Sharar N, Mrahleh MM, Salah B and Awidi A: Generation of a human induced pluripotent stem cell (iPSC) line (JUCTCi011-A) from skin fibroblasts of a healthy Jordanian male subject. Stem Cell Res 48: 101923, 2020.
54. Karam M and Abdelalim EM: Robust and highly efficient protocol for differentiation of human pluripotent stem cells into mesenchymal stem cells. Methods Mol Biol 2454: 257-271, 2022.
55. Sober SA, Darmani H, Alhattab D and Awidi A: Flow cytometric characterization of cell surface markers to differentiate between fibroblasts and mesenchymal stem cells of different origin. Arch Med Sci 19: 1487-1496, 2021.
56. Wang S, Hou Y, Li X, Song Z, Sun B, Li X and Zhang H: Comparison of exosomes derived from induced pluripotent stem cells and mesenchymal stem cells as therapeutic nanoparticles for treatment of corneal epithelial defects. Aging (Albany NY) 12: 19546-19562, 2020.
57. Koliha N, Wiencek Y, Heider U, Jüngst C, Kladt N, Krauthäuser S, Johnston ICD, Bosio A, Schauss A and Wild S: A novel multiplex bead-based platform highlights the diversity of extracellular vesicles. J Extracell Vesicles 5: 29975, 2016.
58. Debacq-Chainiaux F, Erusalimsky JD, Campisi J and Toussaint O: Protocols to detect senescence-associated beta-galactosidase (SA-betagal) activity, a biomarker of senescent cells in culture and in vivo. Nat Protoc 4: 1798-1806, 2009.
59. Zeng ZL and Xie H: Mesenchymal stem cell-derived extracellular vesicles: A possible therapeutic strategy for orthopaedic diseases: A narrative review. Biomater Transl 3: 175-187, 2022.

60. He L, He T, Xing J, Zhou Q, Fan L, Liu C, Chen Y, Wu D, Tian Z, Liu B and Rong L: Bone marrow mesenchymal stem cell-derived exosomes protect cartilage damage and relieve knee osteoarthritis pain in a rat model of osteoarthritis. Stem Cell Res Ther 11: 276, 2020.
61. Zhou X, Liang H, Hu X, An J, Ding S, Yu S, Liu C, Li F and Xu Y: BMSC-derived exosomes from congenital polydactyly tissue alleviate osteoarthritis by promoting chondrocyte proliferation. Cell Death Discov 6: 142, 2020.
62. Zhang F, Guo J, Zhang Z, Qian Y, Wang G, Duan M, Zhao H, Yang Z and Jiang X: Mesenchymal stem cell-derived exosome: A tumor regulator and carrier for targeted tumor therapy. Cancer Lett 526: 29-40, 2022.
63. Jahangiri B, Khalaj-Kondori M, Asadollahi E, Kian Saei A and Sadeghizadeh M: Dual impacts of mesenchymal stem cell-derived exosomes on cancer cells: Unravelling complex interactions. J Cell Commun Signal 17: 1229-1247, 2023.
64. Tan TT, Lai RC, Padmanabhan J, Sim WK, Choo ABH and Lim SK: Assessment of tumorigenic potential in mesenchymal-stem/stromal-cell-derived small extracellular vesicles (MSC-sEV). Pharmaceuticals (Basel) 14: 345, 2021.
65. Heidegger S, Stritzke F, Dahl S, Daßler-Plenker J, Joachim L, Buschmann D, Fan K, Sauer CM, Ludwig N, Winter C, *et al*: Targeting nucleic acid sensors in tumor cells to reprogram biogenesis and RNA cargo of extracellular vesicles for T cell-mediated cancer immunotherapy. Cell Rep Med 4: 101171, 2023.
66. Dominici M, Le Blanc K, Mueller I, Slaper-Cortenbach I, Marini F, Krause D, Deans R, Keating A, Prockop DJ and Horwitz E: Minimal criteria for defining multipotent mesenchymal stromal cells. The international society for cellular therapy position statement. Cytotherapy 8: 315-317, 2006.
67. Maleki M, Ghanbarvand F, Reza Behvarz M, Ejtemaei M and Ghadirkhomi E: Comparison of mesenchymal stem cell markers in multiple human adult stem cells. Int J Stem Cells 7: 118-126, 2014.
68. Willms E, Cabañas C, Mäger I, Wood MJA and Vader P: Extracellular vesicle heterogeneity: Subpopulations, isolation techniques, and diverse functions in cancer progression. Front Immunol 9: 738, 2018.
69. Ekström K, Crescitelli R, Pétursson HI, Johansson J, Lässer C and Olofsson Bagge R: Characterization of surface markers on extracellular vesicles isolated from lymphatic exudate from patients with breast cancer. BMC Cancer 22: 50, 2022.
70. Varderidou-Minasian S and Lorenowicz MJ: Mesenchymal stromal/stem cell-derived extracellular vesicles in tissue repair: Challenges and opportunities. Theranostics 10: 5979-5997, 2020.
71. Yu J, Huang D, Liu H and Cai H: Optimizing conditions of polyethylene glycol precipitation for exosomes isolation from MSCs culture media for regenerative treatment. Biotechnol J 19: e202400374, 2024.
72. Oksvold MP, Neurauter A and Pedersen KW: Magnetic bead-based isolation of exosomes. Methods Mol Biol 1218: 465-481, 2015.
73. Niu Z, Pang RTK, Liu W, Li Q, Cheng R and Yeung WSB: Polymer-based precipitation preserves biological activities of extracellular vesicles from an endometrial cell line. PLoS One 12: e0186534, 2017.
74. Simon L, Lapinte V and Morille M: Exploring the role of polymers to overcome ongoing challenges in the field of extracellular vesicles. J Extracell Vesicles 12: e12386, 2023.
75. Schulz-Siegmund M and Aigner A: Nucleic acid delivery with extracellular vesicles. Adv Drug Deliv Rev 173: 89-111, 2021.
76. Li L, Tian H, Chen Z, Yue W, Li S and Li W: Inhibition of lung cancer cell proliferation mediated by human mesenchymal stem cells. Acta Biochim Biophys Sin (Shanghai) 43: 143-148, 2011.
77. Wu T, Tian Q, Liu R, Xu K, Shi S, Zhang X, Gao L, Yin X, Xu S and Wang P: Inhibitory role of bone marrow mesenchymal stem cells-derived exosome in non-small-cell lung cancer: microRNA-30b-5p, EZH2 and PI3K/AKT pathway. J Cell Mol Med 27: 3526-3538, 2023.
78. Chen R, Liu X and Tan N: Bone marrow mesenchymal stem cell (BMSC)-derived exosomes regulates growth of breast cancer cells mediated by hedgehog signaling pathway. J Biomater Tissue Eng 13: 157-161, 2023.
79. Hu Y, Liu H, Xiao X, Yu Q, Deng R, Hua L, Wang J and Wang X: Bone marrow mesenchymal stem cell-derived exosomes inhibit triple-negative breast cancer cell stemness and metastasis via an ALKBH5-dependent mechanism. Cancers (Basel) 14: 6059, 2022.
80. Liu H, Dilger JP and Lin J: Effects of local anesthetics on cancer cells. Pharmacol Ther 212: 107558, 2020.
81. Maretzky T, Evers A, Zhou W, Swendeman SL, Wong PM, Rafii S, Reiss K and Blobel CP: Migration of growth factor-stimulated epithelial and endothelial cells depends on EGFR transactivation by ADAM17. Nat Commun 2: 229, 2011.
82. Yan M, Yang X, Shen R, Wu C, Wang H, Ye Q, Yang P, Zhang L, Chen M, Wan B, *et al*: miR-146b promotes cell proliferation and increases chemosensitivity, but attenuates cell migration and invasion via FBXL10 in ovarian cancer. Cell Death Dis 9: 1123, 2018.
83. Svensson S, Nilsson K, Ringberg A and Landberg G: Invade or proliferate? Two contrasting events in malignant behavior governed by p16(INK4a) and an intact Rb pathway illustrated by a model system of basal cell carcinoma. Cancer Res 63: 1737-1742, 2003.
84. Evdokimova V, Tognon C, Ng T and Sorensen PH: Reduced proliferation and enhanced migration: Two sides of the same coin? Molecular mechanisms of metastatic progression by YB-1. Cell Cycle 8: 2901-2906, 2009.
85. Ou HL, Hoffmann R, González-López C, Doherty GJ, Korkola JE and Muñoz-Espín D: Cellular senescence in cancer: From mechanisms to detection. Mol Oncol 15: 2634-2671, 2021.
86. Calcinotto A, Kohli J, Zagato E, Pellegrini L, Demaria M and Alimonti A: Cellular senescence: Aging, cancer, and injury. Physiol Rev 99: 1047-1078, 2019.
87. Domen A, Deben C, Verswyvel J, Flieswasser T, Prenen H, Peeters M, Lardon F and Wouters A: Cellular senescence in cancer: Clinical detection and prognostic implications. J Exp Clin Cancer Res 41: 360, 2022.
88. Yaghoubi Y, Movassaghpour A, Zamani M, Talebi M, Mehdizadeh A and Yousefi M: Human umbilical cord mesenchymal stem cells derived-exosomes in diseases treatment. Life Sci 233: 116733, 2019.